Journal of Physics: Conference Series **1435** (2020) 012012 doi:10.1088/1742-6596/1435/1/012012

Particle Polarization and Structure of Vortical Field in Relativistic Heavy-Ion Collisions

Yu. B. Ivanov[1,2,3], **V. D. Toneev**[1] **and A. A. Soldatov**[2]

[1] Bogoliubov Laboratory for Theoretical Physics, Joint Institute for Nuclear Research, Dubna 141980, Russia
[2] National Research Nuclear University "MEPhI", Moscow 115409, Russia
[3] National Research Centre "Kurchatov Institute", Moscow 123182, Russia

E-mail: yivanov@theor.jinr.ru

Abstract. We review studies of vortical motion and the resulting global polarization of Λ and $\bar{\Lambda}$ hyperons in heavy-ion collisions within 3FD model. The 3FD simulations indicate that energy dependence of the observed global polarization of hyperons in the midrapidity region is a consequence of the decrease of the vorticity in the central region with the collision energy rise because of pushing out the vorticity field into the fragmentation regions. At high collision energies this pushing-out results in a peculiar vortical structure consisting of two vortex rings: one ring in the target fragmentation region and another one in the projectile fragmentation region with matter rotation being opposite in these two rings.

1. Introduction

Strongly interacting matter characterized by extremely high baryon and energy densities is created in heavy ion collisions at relativistic energies. This matter demonstrates strong collective behavior that is well described by relativistic hydrodynamics.

Non-central heavy-ion collisions at high energies are also characterized by a huge global angular momentum. This is illustrated in Fig. 1, where the total angular momentum ($J_{\rm total}$) achieved in Au+Au collisions at impact parameter $b = 8$ fm is plotted as a function of the center-of-mass collision energy $\sqrt{s_{NN}}$. The calculations were performed within the model of the three-fluid dynamics (3FD) [1] with two versions of the equation of state (EoS) involving deconfinement transition [2], i.e. a first-order-phase-transition (1PT) EoS and a crossover EoS. As seen, $J_{\rm total}$ rapidly rises with the collision energy, exceeding the value of $10^5\hbar$ at $\sqrt{s_{NN}} > 25$ GeV. It is independent of the used EoS. However, only a part of the total angular momentum is accumulated in the participant region, i.e. in the overlap region of the interacting nuclei, which is of prime interest for us. As seen from Fig. 1, 25–30% of the total angular momentum is deposited into the participant matter in the Au+Au collisions at $b = 8$ fm, which is also a huge amount.

As the angular momentum is accumulated in the participant region, the motion of the matter becomes vortical. It is characterized by the relativistic vorticity

$$\omega_{\mu\nu} = \frac{1}{2}(\partial_\nu u_\mu - \partial_\mu u_\nu), \tag{1}$$

where u_μ is a collective local four-velocity of the matter.

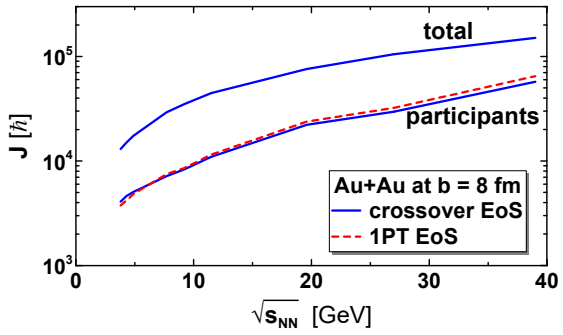

Figure 1. The total angular momentum (conserved quantity) and the angular momentum accumulated in the participant region as functions of $\sqrt{s_{NN}}$.

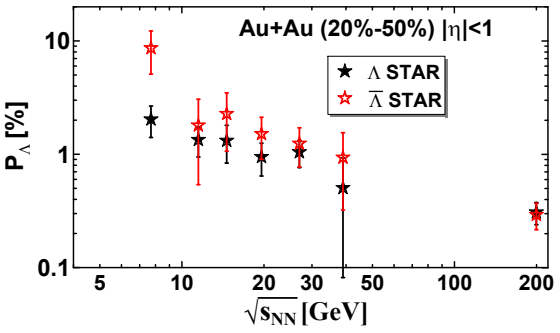

Figure 2. Global polarization of Λ and $\bar{\Lambda}$ as a function of the collision energy $\sqrt{s_{NN}}$ for 20-50% centrality Au+Au collisions.

The vortical motion significantly affects the evolution of the system. However, theoretical and experimental studies of the relevant effects began relatively recently. In particular, in Ref. [3] it was suggested that parton interaction in non-central heavy-ion collisions leads to a global quark polarization along the direction of the global angular momentum. This global polarization is essentially a local manifestation of the global angular momentum of the colliding system through spin-orbital coupling [4, 5]. This phenomenon of the global polarization along the total angular momentum is closely related to the Barnett effect [6] (magnetization by rotation). The Barnett effect consists in transformation of a fraction of the orbital angular momentum associated with the body rotation into spin angular momenta, which, on the average, are directed along the orbital angular momentum.

The most straightforward way to detect the global polarization in relativistic nuclear collisions is based on measuring polarization of Λ hyperons because they are so-called self-analyzing particles. The Λ hyperons weakly decay violating parity. In the Λ rest frame the daughter proton is predominantly emitted along the Λ polarization. Recent measurements by the STAR Collaboration gave nonzero values for the global polarization in the energy range $\sqrt{s_{NN}} = 7.7$–200 GeV [7, 8], see Fig. 2. These results required quantitative approaches to the calculation of the global polarization.

The most popular now thermodynamic approach to such calculations was proposed in Refs. [9, 10] and then further elaborated [11, 12]. More precisely, the derivation of Refs. [9, 10] was performed in terms of the hadronic degrees of freedom and for a (1/2)-spin particle. The thermodynamic approach does not require the precise form of the spin-orbital coupling. It requires only the fact that such a coupling exists and its scale is the strong-interaction one. The latter is required for fast local equilibration of spin degrees of freedom similar to that for momentum degrees of freedom. Nevertheless, certain features of the spin-orbital coupling are silently assumed in the thermodynamic approach. In particular, this coupling is assumed to be the same for baryons and anti-baryons. Had it be a coupling because of induced magnetic field (like in the Barnett effect), polarizations of baryons and anti-baryons would be of opposite sign. All together, this makes possible a definite quantitative estimate of polarization through a suitable extension of the freeze-out formula.

The problem of relation between the vorticity and spin-polarization tensor in relativistic systems is far from being completely solved. The thermodynamic derivation the spin polarization in Refs. [9, 10, 11] is not completely consistent.

In the present paper we review studies of vortical motion and the resulting global polarization

of Λ and $\bar{\Lambda}$ hyperons in Au+Au collisions performed within the 3FD model [14, 15, 16]. The 3FD model describes of the major part of bulk observables, as well as the elliptic and directed flow. We also address the question why does the observed global polarization of hyperons in the midrapidity region, i.e. at pseudorapidity $|\eta| < 1$ (see Fig. 2), drop with the collision energy rise while the angular momentum accumulated in the system substantially increases (see Fig. 1) at the same time?

2. Vorticity in the 3FD model

The 3FD model takes into account a finite stopping power resulting in counterstreaming of leading baryon-rich matter at early stage of nuclear collisions [1]. This nonequilibrium stage is modeled by means of two counterstreaming baryon-rich fluids initially associated with constituent nucleons of the projectile (p) and target (t) nuclei. Later on these fluids may consist of any type of hadrons and/or partons (quarks and gluons), rather than only nucleons. Newly produced particles, dominantly populating the midrapidity region, are associated with a fireball (f) fluid. These fluids are governed by conventional hydrodynamic equations coupled by friction terms in the right-hand sides of the Euler equations. The friction results in energy–momentum loss of the baryon-rich fluids. A part of this loss is transformed into thermal excitation of these fluids, while another part leads to formation of the fireball fluid. Thus, the 3FD approximation is a minimal way to implement the early-stage nonequilibrium of the produced strongly-interacting matter at high collision energies.

Three different equations of state (EoS's) were used in recent simulations: a purely hadronic EoS [17] and two versions of the EoS with the deconfinement transition [2], i.e. a first-order phase transition and a crossover one. In the present review only the first-order-phase-transition (1PT) and crossover EoS's are discussed as the most relevant to various observables.

A so-called thermal vorticity is defined as

$$\varpi_{\mu\nu} = \frac{1}{2}(\partial_\nu \hat{\beta}_\mu - \partial_\mu \hat{\beta}_\nu), \tag{2}$$

where $\hat{\beta}_\mu = \hbar\beta_\mu$, $\beta_\mu = u_\nu/T$, u_μ is collective local four-velocity of the matter, and T is local temperature. In the thermodynamical approach [10, 11, 12] in the leading order in the thermal vorticity it is directly related to the mean spin vector of spin 1/2 particles with four-momentum p, produced around point x on freeze-out hypersurface

$$S^\mu(x,p) = \frac{1}{8m}[1 - n_F(x,p)]\, p_\sigma \epsilon^{\mu\nu\rho\sigma} \varpi_{\rho\nu}(x) \tag{3}$$

where $n_F(x,p)$ is the Fermi-Dirac distribution function and m is mass of the considered particle. To calculate the relativistic mean spin vector of a given particle species with given momentum, the above expression should be integrated over the freeze-out hypersurface. Therefore, we proceed to discussion in terms of the thermal vorticity.

Unlike the conventional hydrodynamics, the system is characterized by three hydrodynamical velocities, u_a^μ (a = p, t and f), in the 3FD model. The counterstreaming of the p and t fluids takes place only at the initial stage of the nuclear collision that lasts from ~ 5 fm/c at $\sqrt{s_{NN}} =$ 5 GeV [14] to ~ 1 fm/c at collision energy of 39 GeV [18]. At later stages the baryon-rich (p and t) fluids have already either partially passed though each other or partially stopped and unified in the central region.

We consider a proper-energy-density weighted vorticity that allows us to suppress contributions of regions of low-density matter. It is appropriate because production of (anti)hyperons under consideration dominantly takes place in highly excited regions of the system. In Fig. 3, the proper-energy-density weighted thermal zx vorticity of the baryon-rich subsystem in the reaction plain (xz) is presented at various time instants in semi-central

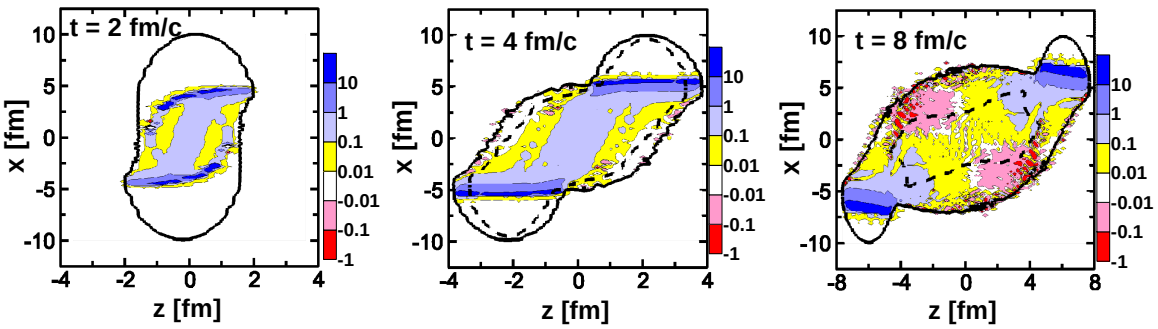

Figure 3. The proper-energy-density weighted thermal zx vorticity of the baryon-rich subsystem, in the reaction plane at various time instants in the semi-central ($b = 6$ fm) Au+Au collision at $\sqrt{s_{NN}} = 7.7$ GeV. Calculations are done with the crossover EoS. z axis is the beam direction. Note different scale along the z axis at different time instants. The outer bold solid contour displays the border of the baryon-rich matter. Inside this contour $n_B/n_0 > 0.1$, where n_B is the proper baryon density and n_0 is the normal nuclear density. The inner bold dashed contour indicates the freeze-out border. Inside this contour the matter still hydrodynamically evolves, while outside – it is frozen out. At $t = 2$ and 4 fm/c there is no frozen-out matter.

($b = 6$ fm) Au+Au collisions at $\sqrt{s_{NN}} = 7.7$ GeV. As seen, the thermal vorticity primarily starts at the border between the participant and spectator matter. Later on it partially spreads to the participant and spectator bulk though remain concentrated near the border. In the conventional hydrodynamics this extension into the bulk of the system is an effect of the shear viscosity. In the 3FD dynamics it is driven by the 3FD dissipation which imitates the effect of the shear viscosity [19]. The spread into the bulk, i.e. into the midrapidity region, is stronger at lower collision energies [14] because of the higher effective shear viscosity than that at higher energies [19]. This explains the drop of the vorticity value and consequently the observed hyperon polarization at the midrapidity with the collision energy rise.

At later times the maximum values in the vortical fields get more and more shifted to the fragmentation regions because of the 1D expansion of the system. At the same time, the vorticity in the participant bulk gradually dissolves. It is peculiarly that four strong oppositely directed vortices are formed at the periphery of the fragmentation regions, see Fig. 3. The vortex at the border with the spectator matter is an order of magnitude stronger than its counterpart. This is the structure as it is seen in the reaction plane.

In fact, in three dimensions these are two vortex rings: one in the target fragmentation region and another in the projectile one. The matter rotation is opposite in these two rings. They are formed because the matter in the vicinity of the beam axis (z) is stronger decelerated because of thicker matter in the center than that at the periphery. Indeed, these rings are formed at the transverse periphery of the stopped matter in the central region. Thus, the peripheral matter acquires a rotational motion. A schematic picture of these vortex rings in the fragmentation regions is presented in Fig. 4.

A similar effect was noticed in the analysis of the vorticity field [20, 21] at lower NICA energies. The authors of Refs. [20, 21] called this specific toroidal structure as a femto-vortex sheet. This femto-vortex sheet is not a ring because the vorticity disappears in the xy plane, i.e. in the plane orthogonal to the reaction xz plane. At higher collision energies this femto-vortex sheet splits into two real rings.

At high collision energies $\sqrt{s_{NN}} > 20$ GeV these rings are also formed in central collisions In fact, the schematic picture of the completely symmetric vortex rings, see Fig. 4, corresponds to the exactly central collision at $b = 0$.

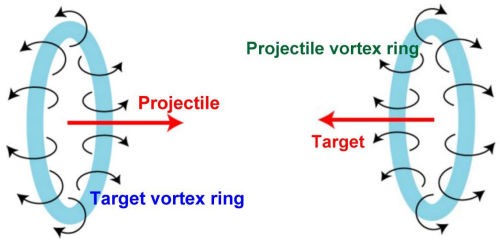

Figure 4. Schematic picture of the vortex rings in the fragmentation regions. Curled arrows indicate direction of the circulation of the target matter.

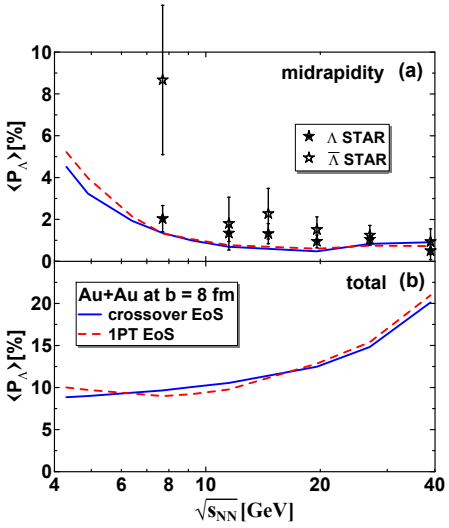

Figure 5. Global (a), i.e. in the central region, and total (b), i.e. averaged over the whole participant region, polarization of Λ hyperons in Au+Au collisions vs collision energy $\sqrt{s_{NN}}$.

3. Polarization

The above observation of pushing out the vortical field to the fragmentation regions has consequence for the polarization of produced particles. The polarized particles dominantly originate from peripheral regions with high vorticity. Therefore, the relative polarization of Λ hyperons should be higher in the fragmentation regions, i.e. the kinematical region of the participant-spectator border, than that in the midrapidity region.

We associate the global midrapidity polarization with the polarization of Λ hyperons emitted from the central region (i.e. central slab) of colliding system, see details in Ref. [16]. Results of the 3FD simulations are presented in panel (a) of Fig. 5. The corresponding 3FD simulations of Au+Au collisions were performed at fixed impact parameters $b = 8$ fm. This value of b was chosen in order to roughly comply with the centrality selection 20-50% in the STAR experiment [7]. As seen from Fig. 5, the 3FD simulations quite satisfactorily reproduce the experimental data, especially the collision-energy dependence of the polarization. This energy dependence is related to the above discussed decrease of the thermal vorticity in the central region with the collision energy rise. The performed estimate predicts that the global midrapidity polarization further increases at NICA/FAIR energies, reaching values of 5% at $\sqrt{s_{NN}} = 3.8$ GeV. This prediction approximately agrees with that made in Ref. [13].

In the case of total Λ polarization, the averaging runs over the whole participant region. Results for the total Λ polarization are presented in panel (b) of Fig. 5. The total Λ polarization increases with collision energy rise. This is in contrast to the energy dependence of the midrapidity polarization. This increase is quite moderate as compared with the rapid rise of the angular momentum accumulated in the participant region, see Fig. 1. The increase of the total polarization with simultaneous decrease of the midrapidity one suggests that the Λ polarization in the fragmentation regions reaches high values at high collision energies. At lower collision energies values of the total and midrapidity polarization are close to each other, which reflects a more homogeneous distribution of the vortical field over the bulk of the produced matter.

4. Summary

3FD calculations of the global polarization of Λ and $\bar{\Lambda}$ hyperons based on the thermodynamics approach are consistent with STAR data. Based on the analysis within the 3FD model [16] predictions are made for the global midrapidity polarization in the FAIR-NICA energy range. We predict that the global midrapidity polarization further increases at NICA/FAIR energies, reaching values of 5% at $\sqrt{s_{NN}} = 3.8$ GeV.

It is found that the energy dependence the observed global polarization of hyperons in the midrapidity region is a consequence of the decrease of the thermal vorticity in the central region with the collision energy rise, which in its turn results from pushing out the vorticity field into the fragmentation regions [15].

At high collision energies $\sqrt{s_{NN}} > 8$ GeV, this pushing-out results in a peculiar vortical structure consisting of two vortex rings: one ring in the target fragmentation region and another one in the projectile fragmentation region with the matter rotation being opposite in these two rings [15], see Fig. 4. These vortex rings produce very strong Λ polarization in the fragmentation regions at noncentral collisions.

Acknowledgments

Fruitful discussions with E. E. Kolomeitsev and O. V. Teryaev are gratefully acknowledged. Y.B.I. was supported by the Russian Science Foundation, Grant No. 17-12-01427, and the Russian Foundation for Basic Research, Grants No. 18-02-40084 and No. 18-02-40085. This work was carried out using computing resources of the federal collective usage center "Complex for simulation and data processing for mega-science facilities" at NRC "Kurchatov Institute", http://ckp.nrcki.ru/.

References

[1] Ivanov Y B, Russkikh V N and Toneev V D 2006 *Phys. Rev.* C **73** 044904
[2] Khvorostukhin A S, Skokov V V, Redlich K and Toneev V D 2006 *Eur. Phys. J.* C **48** 531
[3] Liang Z T and Wang X N 2005 *Phys. Rev. Lett.* **94** 102301, Erratum: [2006 *Phys. Rev. Lett.* **96** 039901]
[4] Betz B, Gyulassy M and Torrieri G 2007 *Phys. Rev.* C **76** 044901
[5] Gao J H, Chen S W, Deng W t, Liang Z T, Wang Q. and Wang X N 2008 *Phys. Rev.* C **77** 044902
[6] Barnett S J 1915 *Phys. Rev.* **6** 239
[7] Adamczyk L *et al.* [STAR Collaboration] 2017 *Nature* **548** 62
[8] Adam J *et al.* [STAR Collaboration] 2018 *Phys. Rev.* C **98** 014910
[9] Becattini F and Piccinini F 2008 *Annals Phys.* **323** 2452
[10] Becattini F, Chandra V, Del Zanna L and Grossi E 2013 *Annals Phys.* **338** 32
[11] Becattini F, Karpenko I, Lisa M, Upsal I and Voloshin S 2017 *Phys. Rev.* C **95** 054902
[12] Fang R h, Pang L g, Wang Q and Wang X n 2016 *Phys. Rev.* C **94** 024904
[13] Baznat M, Gudima K, Sorin A and Teryaev O 2018 *Phys. Rev.* C **97** 041902
[14] Ivanov Y B and Soldatov A A 2017 *Phys. Rev.* C **95** 054915
[15] Ivanov Y B and Soldatov A A 2018 *Phys. Rev.* C **97** 044915
[16] Ivanov Y B, Toneev V D and Soldatov A A 2019 *Phys. Rev.* C **100** 014908
[17] Galitsky V M and Mishustin I N 1979 *Sov. J. Nucl. Phys.* **29** 181
[18] Ivanov Y B and Soldatov A A 2018 *Phys. Rev.* C **97** 021901, *Phys. Rev.* C **98** 014906
[19] Ivanov Y B and Soldatov A A 2016 *Eur. Phys. J.* A **52** 117, *Eur. Phys. J.* A **52** 367
[20] Baznat M I, Gudima K K, Sorin A S and Teryaev O V 2016 *Phys. Rev.* C **93** 031902
[21] Baznat M I, Gudima K K, Sorin A S and Teryaev O V 2013 *Phys. Rev.* C **88** 061901